Soil Biology and Biochemistry 177 (2023) 108911

Contents lists available at ScienceDirect

Soil Biology and Biochemistry

journal homepage: www.elsevier.com/locate/soilbio

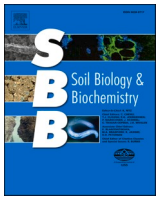

Complex crop rotations improve organic nitrogen cycling

Lauren C. Breza [a,1,*], Maria Mooshammer [c], Timothy M. Bowles [c], Virginia L. Jin [d], Marty R. Schmer [d], Bennett Thompson [a], A. Stuart Grandy [b]

[a] Department of Natural Resources and the Environment, University of New Hampshire, Durham, NH, 03824, USA
[b] Center for Soil Biogeochemistry and Microbial Ecology (Soil BioME), University of New Hampshire, Durham, NH, 03824, USA
[c] Department of Environmental Science, Policy and Management, University of California, Berkeley, Berkeley, CA, 94720, USA
[d] USDA-Agricultural Research Service, Lincoln, NE, 68583, USA

A B S T R A C T

Nitrogen (N) availability in agroecosystems is often poorly coupled to plant N uptake, leading to inefficient fertilizer use and environmental losses. Building soil organic N pools and enhancing internal recycling of N with crop rotations while reducing synthetic inputs may help improve N use efficiency. The organic N pool could be a valuable source of N that could help farmers reduce reliance on large inorganic N inputs if controls on its availability were better understood. While we know that the breakdown of high-molecular weight organic N compounds is the rate-limiting step to accessing bioavailable N from organic sources in natural ecosystems, there has been little work in agroecosystems to identify how management influences this inflection point in the N cycle. To provide insight into how growers can manage the organic N pool to reduce fertilizer input, we examined gross protein depolymerization rates within an agricultural context. Specifically, we investigated 1) how crop rotations affect organic N pools and alter the rate of organic N cycling, and 2) whether inorganic N fertilization enhances, has no effect, or suppresses soil N cycling responses to crop rotation. To test this, we measured gross rates of protein depolymerization, amino acid consumption, mineralization, and ammonium consumption using ^{15}N isotope pool dilution assays on soils collected from a long-term crop complexity experiment near Mead, NE, USA. Treatments sampled included both 0 kg and 180 kg N ha^{-1} fertilization levels in continuous corn, corn-soybean, and corn-soybean-sorghum-oat/clover rotations. We found that higher cropping complexity coupled with zero fertilization increased gross depolymerization and amino acid consumption rates by 193% and 93%, respectively, relative to fertilized, monocrop plots. Gross mineralization was 2.7 and 3.9x higher in complex rotations than corn-soybean and continuous corn rotations, respectively, while ammonium consumption was 4x higher in fertilized plots than unfertilized plots across all cropping regimes. We show that within our study system internal N cycling is stimulated by cropping system complexity; however, N fertilization suppresses some of the benefits of temporal crop diversification. Balancing reduced mineral fertilizer application rates with increased cropping complexity has the potential to promote internal N cycling while minimizing N losses in agroecosystems.

1. Introduction

Modern agriculture relies heavily on synthetic fertilizer to maintain nitrogen (N) availability throughout the growing season and to replace N in harvested biomass. However, fertilizer-intensive practices result in excess N loss, which has serious consequences on the surrounding terrestrial and aquatic ecology and human health. Moreover, excess N exacerbates the effects of climate change by contributing to greenhouse gas emissions (Bodirsky et al., 2012; Velazquez et al., 2016; Vitousek et al., 1997). Simple cropping systems (e.g., one or two rotations) are often found in highly fertile regions where soil organic matter (SOM) content is naturally high. Yet, SOM degradation in these systems over-time results in loss of nutrients, creating a high dependence on external fertilizer inputs that exacerbate environmental N losses (Baumhardt et al., 2015; Doran and Zeiss, 2000; Khan et al., 2007; Kibblewhite et al., 2008). One way to decrease reliance on external N sources is to increase the capacity of internal soil N cycling by building SOM, rather than relying strictly on external N sources. Even in well-fertilized systems, N derived from organic matter, like crop residues and existing soil organic matter (SOM) pools, contributes up to 50% of the bioavailable N (Yan et al., 2019). Designing management plans that augment and utilize internal organic N sources may increase N pools and cycling rates, thereby reducing the need for additional external inputs.

Enhancing crop rotation complexity relies on increasing cash crop diversity and the length of field cover through cover cropping over time (Bowles et al., 2022). Increasing the number of crops in rotation elevates plant functional diversity (i.e., cereal vs legume crop), which increases crop yields (Bowles et al., 2020; Smith et al., 2008) and affects below-ground processes (Bowles et al., 2022; Jilling et al., 2020; Tiemann et al., 2015). Higher crop rotation complexity promotes SOM development

* Corresponding author.
E-mail address: lauren.breza@usda.gov (L.C. Breza).
[1] Present Address: USDA-Agricultural Research Service, National Forage Seed Production Research Unit, 3450 SW Campus Way, Corvallis, OR 97331, USA.

https://doi.org/10.1016/j.soilbio.2022.108911
Received 23 May 2022; Received in revised form 23 November 2022; Accepted 9 December 2022
Available online 10 December 2022
0038-0717/

(Drinkwater et al., 1998; McDaniel et al., 2014b; Mooshammer et al., 2022; Poeplau and Don, 2015), microbial activity (McDaniel et al., 2014b), and improves soil structure (Dexter et al., 2008; Feller and Beare, 1997; King et al., 2020; Six et al., 2000). Because SOM acts as a nutrient reservoir (Wardle et al., 2004). using more complex crop rotations to increase SOM stocks may enhance organic N cycling in agroecosystems.

Increased organic matter provides substrates that fuel microbial N transformations, yet processes that regulate bioavailable N supply remain poorly characterized (Drinkwater and Snapp, 2007). Often overlooked, protein depolymerization (Box 1) precedes N mineralization. Protein depolymerization breaks down large, N-rich organic structures (proteins) into N-bearing monomers (e.g. amino acids) (Schimel and Bennett, 2004). Both plants and microbes rely on free amino acids as valuable N sources (Bardgett et al., 2003; Persson and Näsholm, 2001; Vinolas et al., 2001), especially in N (as well as C) limited soils (Jones and Kielland, 2002). However, the role of amino acids as a N source for crops in agroecosystems remains controversial. Microbes may recycle amino acids by incorporating them into their microbial biomass. In contrast, if microbes do not require this organic N, N mineralization occurs (i.e., microbes release ammonium (NH_4^+) into soil) contributing to the inorganic N pool. Different management practices may influence microbial consumption of amino acids, leading to potentially different fates for N. Depolymerization is a critical step in the N cycle that simultaneously provides N for plant and microbe use, and acts as a gatekeeper for environmental N loss via recycling organic forms of N.

How common agricultural practices affect organic N cycling processes like protein depolymerization, particularly how practices might interact in ways that are complementary or antagonistic for reducing N losses, remains largely contested. Complex cropping systems promote organic N cycling by contributing a diverse profile of organic substrates derived from aboveground biomass, belowground biomass, and root exudates, thus increasing the overall quality and quantity of inputs to the soil. However, complex cropping systems often receive external inorganic N fertilizer in addition to organic N inputs. Thus, our understanding of how external inorganic fertilization affects organic N cycling is limited, making it difficult to predict the supply of N to plants (Farzadfar et al., 2021) and potentially underestimating the amount of bioavailable N generated from organic N cycling (Geisseler et al., 2009; Näsholm et al., 2000; Snapp and Fortuna, 2003).

Ideally, different sources of N – internal organic N cycling and external N inputs – would be complementary such that they combine for an additive or even synergistic effect (e.g., fertilization with inorganic N promotes organic N turnover) (Neff et al., 2002; Norris and Congreves, 2018). On the one hand, supplying N fertilizer may induce C limitation for microbes (Zheng et al., 2020), which would stimulate microbial mineralization of organic matter to obtain more energy (C) and subsequently release more inorganic N (Mooshammer et al., 2014a). As such, fertilization in complex cropping systems could unintentionally result in greater mineralization of inorganic N, increasing potential for N losses and jeopardizing some of the environmental benefits typically associated with crop rotations. Alternatively, high fertilizer additions in complex systems could suppress N mineralization and depolymerization because, under the microbial N mining theory, microbes do not mineralize SOM under high N levels (Geisseler and Horwath, 2008; Mahal et al., 2019; Moorhead and Sinsabaugh, 2006). However, the interactive impacts of management practices such as crop rotation and fertilization on depolymerization, amino acid consumption, mineralization, and immobilization, remain uncertain, especially systems under moderate or low rates of synthetic N inputs.

We now have the ability to address this knowledge gap with the recent optimization of isotope pool dilution (IPD) methods to measure amino acid flux in soils and decomposing litter (Wanek et al., 2010). Originally developed by Kirkham and Bartholomew (1954) to estimate inorganic N fluxes, newer assays can quantify gross amino acid production (i.e., depolymerization) and consumption. Quantifying amino acid flux combined with measurements of inorganic N flux (i.e., mineralization and immobilization) can offer mechanistic explanations for N transformations in response to management practices in agroecosystems.

The overall objective of this study was to understand how complex crop rotations change soil microbial activity, SOM dynamics and organic N cycling and how external N fertilizer moderates these impacts. We studied a long-term agricultural research experiment evaluating crop rotation complexity and N management and used ^{15}N-amino acid pool dilution techniques to answer: 1) how do more complex crop rotations affect organic N pools and organic N cycling; and 2) does inorganic N enhance, suppress, or have no effect on soil organic N cycling responses to complex crop rotations?

2. Materials and methods

2.1. Field site

Soils were collected in June 2018 from the University of Nebraska-Lincoln's Eastern Nebraska Research and Extension Center (ENREC) near Mead, NE. The experiment was established on Yutan silty clay loam-Tomek silt loam complex. The field site elevation is 366 m and mean annual temperature and precipitation is 10.5 °C and 765 mm, respectively. The crop rotation experiment is a split plot factorial design, with crop complexity as the main plot and N fertilizer as the split plot. Plots are 9 m wide and 10 m long and replicated across five main blocks. The crop complexity experiment was established in 1972 and fertilizer treatments were introduced in 1984 (Sindelar et al., 2016). The plots were disked annually, twice in the spring from 1983 until 2006; in 2007, the study was converted to no-till. We collected soils from four of the five replicated blocks from the following crop rotations: continuous corn (*Zea mays*; low complexity), corn-soybean (*Glycine* max (L.) Merr; medium complexity), and corn-soybean-sorghum-oat/clover mixture

Box 1
Identified and defined terms used throughout this study.

1. **Gross depolymerization** (GD) – Total amount of amino acids generated via the breakdown of protein structures.
2. **Gross amino acid consumption** (GC) – Total amount of amino acids consumed by microbes.
3. **Net depolymerization** (ND) – Total amount of amino acids left over in the soil after accounting for amino acid consumption. (ND = GD – GC)
4. **Gross mineralization** (N_{min}) – Total amount of ammonium produced by microbes.
5. **Gross immobilization** (N_{imm}) – Total amount of ammonium consumed by microbes.
6. **Net mineralization** (N_{net}) – Total amount of ammonium left over in the soil after accounting for immobilization. ($N_{net} = N_{min} - N_{imm}$)
7. **Amino acid cycling** – The production and consumption of amino acids in the soil by microbes.
8. **Internal nitrogen cycling** – Organic nitrogen derived from crop residue input that is transformed into bioavailable forms of organic and inorganic N via microbial pathways.

(*Sorghum bicolor* (L.) Moench; *Avena sativa* L.; 80% *Melilotus officinalis* (L.) Lam. + 20% *Trifolium pratense* L.; high complexity). Crop residues from each treatment are left in the field and no removal occurs. Corn and sorghum residues are stalk chopped into smaller pieces to improve planting conditions and increase the residue-to-soil contact.

Soils were collected during the corn phase of each rotation during mid vegetative growth. Fertilized subplots receive fertilizer N as granular urea (46-0-0) that is manually broadcast applied without incorporation and application dates were contingent on favorable soil conditions for field access (Sindelar et al., 2016). Fertilizer rates for the corn and grain sorghum phases of the rotation were 0, 90, and 180 kg N^{-1} ha and 0, 34, and 69 kg N^{-1} ha for the soybean and oat/clover phases. We utilized the zero (0 kg N^{-1} ha) and high (180 kg N^{-1} ha) fertilizer subplots from the continuous corn, corn-soybean, and complex cropping systems. The high fertilizer treatment falls above the rainfed fertilization rate for the region, (Tenorio et al., 2020). We opted to use the zero and high fertilizer treatments to capture N flux responses on either end of the fertilizer application spectrum.

2.2. Soil characterization

Intact bulk soil (0–15 cm) was extracted by hammer core (5.8 cm diameter) lined with a plastic sleeve to minimize soil disturbance. Soils were immediately placed on ice and shipped to the University of New Hampshire (UNH), Durham and University of California, Berkeley. In the lab, soil cores were homogenized and passed through a 1 cm mesh sieve to remove large debris, then subsampled for immediate initiation of laboratory analyses where soils were further sieved according to specific procedural requirements. Microbial biomass C and N was measured by the chloroform fumigation extraction method (Vance et al., 1987). Dissolved organic carbon (DOC) was determined via UV/persulfate digestion on a TOC analyzer. Total dissolved nitrogen (TDN) was measured using the alkaline persulfate digestion method (Yu et al., 1994). Extractable ammonium and nitrate concentration were quantified by colorimetric procedures as described in Hood-Nowotny et al. (2010). The total free amino acid pool was quantified by the fluorometric OPAME procedure based on Jones et al. (2002). Total soil C and N content was determined by dry combustion using an elemental analyzer (Costech ECS 4010 CHNSO elemental analyzer). Protein content, a soil health indicator of potentially available organic nitrogen, was measured according to Hurisso et al. (2018). Gross N transformation rates were measured at the UNH soil biogeochemistry lab as detailed in sections 2.3 and 2.4.

2.3. Gross depolymerization

We modified a GC-MS ^{15}N pool dilution method introduced by Wanek et al. (2010) to quantify gross rates of protein depolymerization. The original method was designed to measure protein depolymerization rates on decaying litter and, more recently, has been modified for use on soils (Noll et al., 2019a; Wild et al., 2013). Our approach differs from previous versions of the method in that we used a different derivatization step. This allowed us to improve the sensitivity of the assay with use on mineral soils so that we could measure amino acid production and consumption in agricultural soils under varying management practices.

Field moist soil samples were weighed to 6 g in duplicate pairs (i.e., t_0 and t_1) and were pre-incubated for 48 h at ambient temperature under vented conditions. A cell-free, ^{15}N labeled amino acid solution (98 atom % ^{15}N, 20 mM in water, Sigma-Aldrich, 767972-1 EA, Lot # MBBC1096) representing 20% of the average amino acid pool based on a random subsample of the soils was added to each sample duplicate. In preliminary IPD trials, Wanek et al. (2010) found that excessive additions of amino acids (>25% of the background pool) triggered strong microbial consumption of amino acids and stimulated activity. Therefore, we opted to increase the amino acid pool by 20% to avoid priming the microbial community, but still provide sufficient levels of detection.

Ultrapure water was added in very small increments for a total of 0.5–1 mL to each soil duplicate to achieve ~60% of field capacity. Field capacity was determined by saturating a small amount of soil with water and allowing it to drip under negative pressure until water stopped flowing. After water stopped flowing, the water content of the saturated soil was determined gravimetrically. Soil saturation is important for aiding in the full distribution and suspension of the isotopic label throughout the soil. After the addition of the isotopic label, soils were incubated for 10 (t_0) and 30 (t_1) minutes, with the measurable rate of proteolysis occurring during a 20-min timeframe. At each time point, the respective duplicates received 20 mL of "stop solution" consisting of 10 mM calcium sulfate ($CaSO_4$) and 37% formaldehyde (CH_2O). $CaSO_4$ is the amino acid extraction agent, while formaldehyde inhibits microbial activity, production of additional extracellular enzymes, and denatures the existing extracellular enzymes, thereby halting further proteolysis.

A "recovery" amino acid mixture was prepared, consisting of 0.05% of each individual amino acid by mass (18 in total, Sigma-Aldrich, L-Amino acids, LAA21-1 kt, Lot # SLBN7211V); 20 μL of the amino acid recovery mixture was mixed with 500 μL of 10 mM $CaSO_4$and 20 mL of stop solution to establish amino acid recovery standards. The amino acid recovery standards followed soil samples in parallel throughout the amino acid extraction and derivatization process. A true blank was created by mixing 500 μL of 10 mM $CaSO_4$ and 20 mL of stop solution, which also followed the soil samples and amino acid recovery standards through each step in the assay.

2.3.1. Amino acid extraction from soil

After terminating the incubation, all samples, blanks, and recovery standards were placed on an orbital shaker for 5 min at 200 rpm, then centrifuged at 10,000 rpm for 5 min. Samples were kept at room temperature during shaking and centrifuging. The supernatant was poured off into a 30 mL syringe attached to a filtering apparatus and the filtrate was passed through a cation exchange cartridge (CEC) and captured in a 50 mL tube. We constructed a filtering apparatus by attaching a 25 mm diameter disposable syringe filter device (Whatman glass microfiber filter with polypropylene housing, pore size 1.2 μm, Cat No. 6886-2512) to a 30 mL Luer lock syringe (Wanek et al., 2010). Amino acid extracts were loaded onto CECs and afterwards the cartridges were rinsed with ultra-pure water to remove any residual formaldehyde from the extract solution. Amino acids were eluted from the CECs with 3M NH_3 and the eluent was collected in glass vials. Ammonia was used as the eluent because it titrates the net positively charged amino acids to their anionic forms, allowing for amino acid removal from the resin, and the volatile nature of NH_3 permitted evaporation under an N_2 dryer (Wanek et al., 2010). The eluent was dried under N_2 until all the NH_3 evaporated, leaving behind dried amino acids. The dried residue was reconstituted, and side walls of the vials rinsed with a 20% ethanol solution. The resulting amino acid-ethanol solution was transferred via pipette into 2 mL snap-cap tubes and dried again under N_2 which were then stored at −20 °C until derivatized for analysis.

We prepared all cation exchange cartridges (CECs) by attaching CEC's to a 30 mL Luer lock syringe, adding 10 mL of ultra-pure water into the syringe (carefully replacing the plunger), and allowing the water to drip slowly through the CECs over a 3 h period, taking care to retain water in the CECs at the end of the 3 h soak (Wanek et al., 2010). Cation exchange cartridges should not be allowed to dry out after the initial soak. This process ensures that the CEC resin beads are fully saturated prior to conditioning with reagents. After the initial soak, CECs were sequentially rinsed with 10 mL of 3M ammonia (NH_3), 10 mL of ultra-pure water, 10 mL of 1M HCl, and finally 10 mL of ultra-pure water, again taking care to retain solutions within the CEC as to not allow them to dry out. This process removes any contamination by amino acids and regenerates the charge of the resin (Wanek et al., 2010).

2.3.2. Derivatization

A derivatization step is necessary to separate amino acids by gas

chromatography (Hušek, 1991). We adopted the derivatization procedure described in Chen et al. (2010) which uses methylchloroformate (MCF) as the primary derivatization solvent. We added an internal amino acid solution to evaluate the amino acid recovery through the derivatization process. The internal amino acid solution consisted of 0.1% norvaline and 0.1% norleucine. To complete the derivatization process, dried amino acid samples, blanks, and recovery standards were dissolved in 240 μL of a 1:1 solution of 8 M ammonium hydroxide (NH_4OH): methanol. Unless otherwise noted, pure forms of reagents were used for the derivatization step. The derivatization reagents, 100 μL pyridine, 100 μL MCF, 180 μL chloroform, and 180 μL 50 mM sodium carbonate ($NaCO_3$), were added (in that order) to each snap-cap tube to complete a series of methylation reactions that yielded derivatized forms of amino acids. The bottom chloroform phase was extracted from the snap-cap and transferred to a glass gas chromatograph (GC) insert containing sodium sulfate ($NaSO_4$) for analysis. Standard curves and blanks were derivatized alongside samples. All samples, blanks, and standards were immediately run using a gas chromatograph-mass spectrometer (GCMS) after the completion of the derivatization step.

Derivatized blanks were used to determine the method detection limit (MDL) and method quantitation limit (MQL) for each amino acid. Derivatized standards and recoveries were used to correct the measured concentration of each amino acid. Upon the completion of post processing the data, amino acid concentrations were determined and rates of gross protein depolymerization (GD) and gross amino acid consumption (GC) were calculated using Equations (1) and (2), respectively, which are analogous to the pool dilution equations developed by Kirkham and Bartholomew (1954).

$$GD = \frac{(N_{t2} - N_{t1})}{(t_2 - t_1)} \times \left(1 + \frac{ln\left({}^{\%at}{}^{15}N_{t2} - {}^{\%at}{}^{15}N_{tb}\right) \div \left({}^{\%at}{}^{15}N_{t1} - {}^{\%at}{}^{15}N_{tb}\right)}{ln\,(N_{t2} \div N_{t1})}\right) \quad (1)$$

$$GC = \frac{(N_{t2} - N_{t1})}{(t_2 - t_1)} \times \frac{ln\left({}^{\%at}{}^{15}N_{t1} - {}^{\%at}{}^{15}N_{tb}\right) \div \left({}^{\%at}{}^{15}N_{t2} - {}^{\%at}{}^{15}N_{tb}\right)}{ln\,(N_{t2} \div N_{t1})} \quad (2)$$

Where, N_t is the concentration of the unlabeled amino acid fraction (mg N/kg dry wt) at t_1 or t_2, $\%at^{15}N_t$ is the concentration of the labeled amino acid fraction at t_1 or t_2, and $\%at^{15}N_b$ is the concentration of the background ^{15}N abundance (a constant, 0.366 at%^{15}N). These equations follow first order kinetics and can expect exponential decline of amino acid concentrations through time. Amino acid mean residence time (MRT) was calculated by dividing the total amino acid pool size by influx and efflux rates; Mooshammer et al., (2012). Higher MRT indicates slower amino acid cycling (i.e., amino acids remain in the soil longer), while lower MRT points to rapid amino acid cycling in the soil.

2.4. NH_4^+ mineralization pool dilution

Gross NH_4^+ mineralization was determined by a ^{15}N pool dilution assay (Hood-Nowotny et al., 2010). ^{15}N-labeled NH_4^+ was added to the soil and measured after 4 (t_0) and 24 (t_1) hours. Over time, ^{15}N abundance is diluted as unlabeled NH_4^+ produced from organic N through mineralization. To determine the amount of ^{15}N label necessary to add to each sample (~20% of the background NH_4^+ pool), we measured the NH_4^+ concentration of soils via a colorimetric assay (Hood-Nowotny et al., 2010; Kandeler and Gerber, 1988). Given that half of the soils were fertilized, we adjusted the quantity of ^{15}N label for fertilized soils. Four grams of each soil sample were weighed out in duplicates (t_0 and t_1) into 50 mL plastic tubes and a 0.25 mM ^{15}N tracer solution (Ammonium-^{15}N chloride, 10 atom%, ^{15}N, Sigma-Aldrich 348465-25G, Lot # TA1688V) was added to each sample pair. The exact weight of each soil was noted. We added 1.2 mL of ultrapure water to the unfertilized soil to account for the differences in moisture content caused by the increased volume of ^{15}N label in the fertilized soils. After addition of the tracer, soils were vigorously shaken to homogenize the tracer throughout the sample. Samples were incubated at room temperature for four and 24 h. The incubation was terminated by adding 30 mL of 1 M KCl solution. Samples were shaken for 30 min at 200 RPM to extract NH_4^+ from the soils. Soil slurries were passed through an ashless filter (Whatman, no. 40, Cat No. 1440-110) and extracts captured in 20 mL plastic vials.

Extracts underwent a microdiffusion to determine the NH_4^+ concentration of the labeled samples. Plastic scintillation vials (20 mL volume) received 100 mg of MgO plus 10 mL soil extract. Blank diffusions were also prepared using 10 mL of 1M KCl extractant instead of soil extract. One acid trap was immediately added to each vial, and in the case of expected high concentrations of NH_4^+ two acids traps were added. Acid traps consisted of 1 cm discs constructed from ashless filter paper (Whatman, no. 40, Cat No. 1440-110) that were encapsulated in Teflon tape. Scintillation vials were sealed and shaken for 48 h. After the diffusion, acid traps were removed from the scintillation vials, placed into a 1.5 mL snap-cap tube, and dried in a desiccator for 48 h. Dried filter discs were removed from the Teflon tape and transferred into tin capsules for stable isotope analysis using isotope ratio mass spectrometry (IRMS) performed by the Cornell Stable Isotope Laboratory. Samples that fell below the expected range for IRMS analysis received an unlabeled N spike of 71 mM L-Proline (Sigma-Aldrich, P0380-1 G, Lot #SLBL4766V) so that there was optimal N content for detection. We assumed the natural abundance of ^{15}N in the unlabeled proline is negligible in our calculations. Gross NH_4^+ production ($N_{min.}$) and gross NH_4^+ consumption ($N_{imm.}$) were calculated using Equations (3) and (4), respectively.

$$N_{min.} = \frac{(C_{t2} - C_{t1})}{(t_2 - t_1)} \times \left(\frac{ln[APE_{t1} \div APE_{t2}]}{ln\,(C_{t2} \div C_{t1})}\right) \quad (3)$$

$$N_{imm.} = \frac{(C_{t1} - C_{t2})}{(t_2 - t_1)} \times \left(1 + \frac{ln[APE_{t2} \div APE_{t1}]}{ln\,(C_{t2} \div C_{t1})}\right) \quad (4)$$

Where C_{t1} and C_{t2} is the amount of N (μg N g-1 dry soil) at t_1 and t_2, APE_{t1} and APE_{t2} is the atom percent excess at t_1 and t_2 defined as $at\%\ ^{15}N_{sample} - at\%\ ^{15}N_{background}$, and t_1 and t_2 are the times (days) when the pool dilution assay was stopped.

2.5. Extracellular enzyme assays

Potential extracellular hydrolytic and oxidative enzyme activities were determined fluorimetrically and photometrically, respectively, according to standard assays (Bach et al., 2013; German et al., 2011). For the determination of 1,4-β-cellobiosidase (CBH), β-glucosidase (BG), exochitinase (N-acetly-glucosaminidase; NAG), and acid phosphatase (PHO), we used methylumbelliferone (MUF)-linked substrates. Leucine aminopeptidase (LAP) was measured by using L-leucine-7-amido-4methylcoumarin (AMC) as a substrate. For the oxidative enzyme activity assays (peroxidase (PER) and phenol oxidase (PPO)), we used L-3, 4-dihydroxyphenylalanine (L-DOPA) as a substrate.

2.6. Statistical analysis

We used R statistical software (R Core Team, 2020) with *lme4* (Bates et al., 2015) to perform a linear mixed-effects, two-way analysis of variance (ANOVA) to determine differences between cropping systems and fertilized plots for amino acid flux rates, mean residence times, NH_4^+ flux rates, enzyme activities, and soil chemistry. Treatment blocks ($n = 4$) were designated as random effects, with cropping system nested within block, and cropping system and N fertilization designated as fixed effects. The data were not normally distributed for amino acid mean residence times and NH_4^+ fluxes and were log transformed. We calculated the estimated marginal means (Lenth, 2020) for our mixed effects models to determine pairwise differences between each main effect treatment combinations that had significant interaction effects.

Nonmetric multidimensional scaling (NMDS) was used to explore patterns among treatments for indicators of biogeochemical functioning and measures of microbial enzyme activity in multivariate sampling space (Oksanen et al., 2020). We use the Sorensen (Bray-Curtis) index for the distance measure used in the NMDS ordination. The final NMDS solution was accepted if the stress value was less than 0.2. We conducted a permutational multivariate analysis of variance (PERMANOVA) to determine whether ordination groupings were statistically different from one another. We tested for homogeneity of dispersion across groups using the betadisp function and accepted the null hypothesis of homogeneity of group dispersions (Anderson and Walsh, 2013). Significance of correlations was tested with 999 permutations. All plots were generated using the package ggplot2 (Wickham, 2020).

3. Results

3.1. Amino acid flux

We found an interaction between cropping system and fertilizer inputs for gross protein depolymerization ($p = 0.03$) (Fig. 1a) and gross amino acid consumption ($p < 0.001$) rates (Fig. 1b). Fertilization reduced depolymerization rates by 2x and 3.3x in the continuous corn and complex rotations, respectively, but not in the corn-soybean rotation. Similar patterns emerged with gross amino acid consumption rates; fertilization reduced amino acid consumption by 1.5x and 3.7x in the continuous corn and complex rotations, respectively, but not in the corn-soybean rotation. Amino acid MRT was not affected by the main effects of fertilizer treatment and cropping system; however, there was a significant interaction of fertilizer treatment and cropping system (Fig. 1C; $p = 0.024$). Fertilized continuous corn plots had significantly higher MRT than the fertilized corn-soybean system and the unfertilized complex system.

3.2. Ammonium flux

Agricultural management impacted gross NH_4^+ mineralization rates (Fig. 2), including an interaction between cropping complexity and fertilizer ($p = 0.01$). The continuous corn cropping system had the lowest mineralization rates, compared to the other two cropping system treatments. Within the continuous corn treatment, there were lower mineralization rates under the high fertilizer treatment compared to the unfertilized treatment. There was no interaction effect for NH_4^+ immobilization rates, however we found that fertilizer increased immobilization rates relative to the unfertilized treatment ($p < 0.001$). Finally, we found no differences in NH_4^+ MRT between treatments.

3.3. Overall biogeochemical response to management

Cropping system complexity and fertilizer treatments each drove differences in soil C concentration, but there was no interaction between management treatments (Table 1). Complex cropping systems had greater total soil C than corn-soybean or continuous corn systems ($p = 0.01$). Fertilization increased both soil C ($p = 0.02$) and N ($p < 0.001$) relative to zero fertilizer inputs, regardless of cropping system. Additionally, fertilization increased dissolved organic carbon (DOC) compared to zero fertilizer inputs ($p = 0.01$), whereas cropping system complexity increased POXC content in the complex system compared to the continuous corn system ($p = 0.01$). An interaction between cropping complexity and fertilizer influenced soil pH; pH was higher in all unfertilized plots when compared to fertilized plots and was significantly lower in the continuous corn x high fertilizer treatment ($p < 0.001$; SI Fig. 1). Gross depolymerization was weakly, positively correlated with pH ($p = 0.05$; $R^2 = 0.12$). There were no significant correlations between pH and gross amino acid consumption, mineralization, or immobilization.

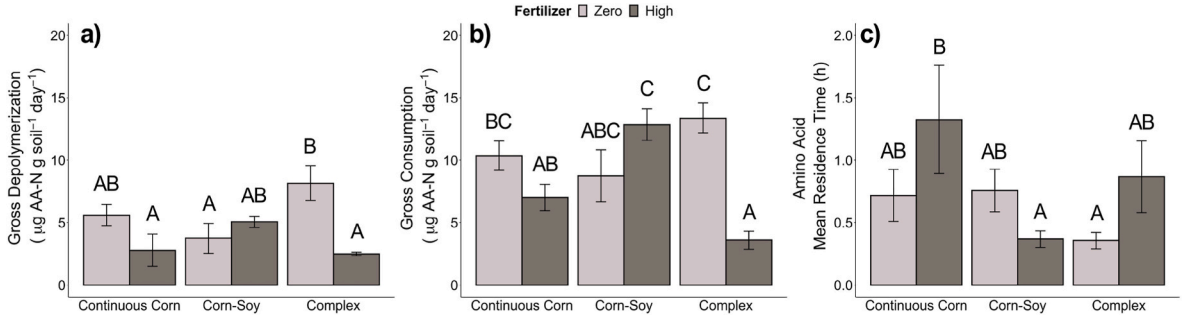

Fig. 1. Amino acid flux in response to fertilizer and crop rotation complexity. Letters denote significant interactions across all treatments. Full ANOVA results in Table 1.

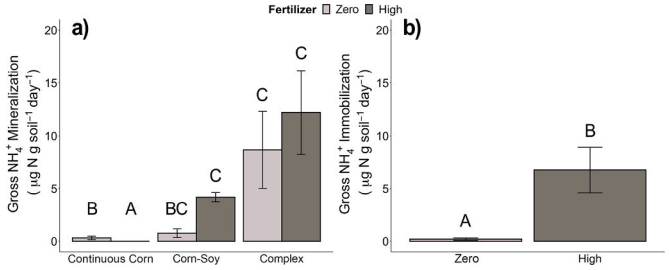

Fig. 2. Ammonium flux in response to fertilizer and crop rotation complexity. Letters denote significant interactions across all treatments (panel a) and significant differences between zero and high fertilized plots (panel b). Full ANOVA results in Table 1.

Table 1
Soil flux, chemical property, and extra cellular enzyme activities (mean ± s.e., n = 4) and the effects of crop rotational diversity (C), fertilizer rate (FR), and their interactions (C x F) derived from a mixed model ANOVA. Abbreviations: amino acid mean residence time (AA MRT); NH_4^+ mean residence time (NH_4^+); total dissolved nitrogen (TDN); dissolved organic carbon (DOC); Permanganate oxidizable carbon (POXC); β-glucosidase (BG); 1,4-β-cellobiosidase (CBH); exochitinase (N-acetyl-glucosaminidase; NAG); leucine aminopeptidase (LAP); phenol oxidase (PPO); peroxidase (PER); microbial biomass carbon (MBC); microbial biomass N (MBN); microbial biomass mean residence time (MB MRT).

Variable	Units	Continuous Corn		Corn-Soybean		Complex		F Statistic		
		Zero	High	Zero	High	Zero	High	C	FR	C x FR
Gross Depolymerization	μg AA-N g^{-1} dw d^{-1}	5.6 ± 1.7	2.8 ± 2.6	3.7 ± 2.4	5.1 ± 0.9	8.2 ± 2.8	2.5 ± 0.3	0.4	**8.7** *	**6.5** *
Gross Consumption	μg AA-N g^{-1} dw d^{-1}	10.4 ± 1.2	7.0 ± 1.1	8.7 ± 2.1	12.8 ± 1.3	13.4 ± 1.2	3.6 ± 0.7	2.3	**9.0** **	**15.8** ***
AA MRT	H	0.7 ± 0.4	1.3 ± 0.9	0.8 ± 0.3	0.4 ± 0.1	0.4 ± 0.1	0.9 ± 0.6	3.1	1.5	**5.7** *
N Mineralization	μg N g^{-1} dw d^{-1}	0.3 ± 0.2	0 ± 0	0.8 ± 0.4	4.2 ± 0.4	8.7 ± 3.6	12.2 ± 4	**25.6** ***	2.4	**8.5** **
N Immobilization	μg N g^{-1} dw d^{-1}	0.4 ± 0.3	2.7 ± 1.3	0.1 ± 0.1	4.4 ± 1.5	0.1 ± 0.1	13.1 ± 5.1	0.1	**13.4** ***	0.9
NH_4^+ MRT	H	2.3 ± 0.5	0 ± 1.2	1.3 ± 0.3	0 ± 0.2	0.5 ± 0.8	0 ± 0.5	0.8	0.3	0.01
C	%	1.4 ± 0.12	1.71 ± 0.11	1.47 ± 0.09	1.58 ± 0.08	1.83 ± 0.04	1.97 ± 0.1	**7.5** *	**8.1** *	0.8
N	%	0.14 ± 0.01	0.17 ± 0.01	0.14 ± 0.01	0.16 ± 0	0.17 ± 0	0.19 ± 0.01	**11.7** ***	**18.1** ***	1.1
TDN	μmol N g^{-1} dw	0.2 ± 0.1	1.7 ± 0.2	0.5 ± 0.1	1.6 ± 0.6	0.6 ± 0.1	2.3 ± 0.6	0.9	**23.2** ***	0.3
DOC	μmol C g^{-1} dw	6.3 ± 0.2	9.5 ± 0.2	6.4 ± 0.3	7.4 ± 0.4	6.8 ± 0.3	9.2 ± 2.0	0.9	**9.6**	0.8
POXC	μg g^{-1} dw	398 ± 52	497 ± 49	474 ± 50	502 ± 51	639 ± 33	655 ± 40	**8.2**	1.8	0.5
NH_4^+	μmol NH_4^+ g^{-1} dw	0.77 ± 0.16	0.12 ± 0.01	0.29 ± 0.15	0.07 ± 0.01	0.18 ± 0.05	0.09 ± 0.03	**5.8** *	**17.7** ***	**5** *
NO_3^-	μmol NO_3^- g^{-1} dw	0.97 ± 0.21	0.18 ± 0.03	1.42 ± 0.42	0.32 ± 0.03	1.77 ± 0.44	0.35 ± 0.07	1.6	**25.6** ***	0.7
BG	nmol g^{-1} dw h^{-1}	508 ± 63	537 ± 114	635 ± 115	746 ± 119	1017 ± 96	1014 ± 62	**10.6** **	0.5	0.2
CBH	nmol g^{-1} dw h^{-1}	89 ± 5	110 ± 25	129 ± 39	192 ± 43	258 ± 48	246 ± 21	**9.2** **	1.1	0.9
NAG	nmol g^{-1} dw h^{-1}	213 ± 23	277 ± 45	266 ± 61	234 ± 28	332 ± 29	284 ± 38	1.2	0.03	1.6
LAP	nmol g^{-1} dw h^{-1}	34.5 ± 11.6	21.3 ± 8.28	21 ± 4.73	17.3 ± 3.71	43.5 ± 8.57	37.8 ± 10.6	3.1	1.3	0.2
PPO	μmol g^{-1} dw h^{-1}	0.25 ± 0.02	0.46 ± 0.04	0.26 ± 0.02	0.27 ± 0.02	0.28 ± 0.02	0.31 ± 0.02	2.4	**48** ***	**25.4** ***
PER	μmol g^{-1} dw h^{-1}	0.98 ± 0.06	2.13 ± 0.20	0.91 ± 0.04	1.15 ± 0.08	0.97 ± 0.03	1.26 ± 0.16	**8.2** *	**92.5** ***	**16.1** ***
MBC	μmol C g^{-1} dw	10.6 ± 0.6	10.4 ± 1.5	13 ± 1.5	11.8 ± 0.9	17.6 ± 1.5	10.4 ± 1.6	**4.4** *	**9** **	**5.1** *
MBN	μmol N g^{-1} dw	1.4 ± 0.1	0.9 ± 0.2	1.3 ± 0.2	1 ± 0.2	1.9 ± 0.3	1.3 ± 0.1	3.0	**11.2** **	0.8
MB MRT	H	111 ± 16	71 ± 7	89 ± 7	115 ± 15	119 ± 11	92 ± 10	0.9	2.0	**4.5** *

Significant results indicated by: • p = 0.05; *p < 0.05; **p < 0.01; ***p < 0.001.

Unsurprisingly, fertilization influenced inorganic N (NH_4^+ and NO_3^-) and TDN. Total dissolved N ($p < 0.001$) and NO_3^- ($p = 0.001$) were both ~5x higher ($p = 0.001$) in fertilized plots than in unfertilized plots. We found an interaction between rotation and fertilization for NH_4^+ concentration ($p = 0.04$). Soil NH_4^+ concentration was 4.5–8.5x higher in the fertilized, continuous corn plots than in any other treatment combination.

Carbon acquiring enzymes, beta-glucosidase (BG) and cellobiohydrolase (CBH), were significantly affected by cropping system, with both enzymes exhibiting higher activity in the more complex system (Table 1). In the complex system, BG activity was 2x higher ($p = 0.01$) and CBH activity was 2.5x higher ($p = 0.01$) than the continuous corn treatments. We found no differences between treatments for N acquiring enzymes NAG and LAP. However, we found interaction between fertilization and crop rotation that influenced C degrading enzymes phenoloxidase (PPO) and peroxidase (PER). Both PPO ($p < 0.001$) and PER ($p = 0.01$) activity was nearly twice as high in continuous corn plots that received fertilizer than any other treatment combination.

There was an interactive effect between cropping system complexity and fertilizer treatment on microbial biomass C (Table 1, $p = 0.02$). Microbial biomass C was highest in the complex cropping system that received zero fertilizer compared to every other treatment combination, except the zero fertilizer, corn-soybean treatment. Fertilizer influenced microbial biomass N ($p = 0.01$); overall, there was higher microbial biomass N in the zero fertilizer plots, regardless of cropping system complexity (Table 1).

We used non-metric multidimensional scaling (NMDS) to visualize how N transformations, soil C and N pools, and soil enzyme activities (i.e., all variables in Table 1) varied together across the cropping system and fertilization. The stress score of 0.12 indicated that the two-dimensional space represented the data sufficiently well. Each variable's vector length and direction indicate the strength of the variable's association with the NMDS axes; only variables that were significantly associated with the NMDS axes were included in the ordination space. The ordination demonstrates a distinct separation between fertilizer treatments and cropping systems. There was a greater separation of continuous corn from the other cropping systems under high fertilizer, and less separation among cropping systems under zero fertilizer, which suggests that rotating crops (two or more) mitigates the impact of fertilizer addition on soil function. Variables indicating microbial activity and N cycling processes tracked strongly with complex cropping systems. We found that indicators of biogeochemical functioning varied among the different cropping systems (PERMANOVA, $p = 0.003$, Fig. 3 and SI Table 2). However, there was not a significant effect of fertilizer ($p = 0.393$) and there was no interaction between fertilizer treatments and crop rotational diversity ($p = 0.857$).

4. Discussion

Our study uses a novel application of amino acid pool dilution approaches to show that fertilization modulates the positive effects of crop rotational complexity on organic N cycling. We found that fertilizer inputs suppressed organic N processing, reducing the potential benefits of greater organic N turnover provided by more complex cropping systems. High external N additions alter internal soil organic N cycling, likely by disincentivizing microbial processing of proteins, oligopeptides, and amino acids to obtain bioavailable N from organic sources, resulting in diminished rates of depolymerization (Hu et al., 2016; Moorhead and Sinsabaugh, 2006; Noll et al., 2019b; Schimel and Bennett, 2004). However, we did not find differences in depolymerization

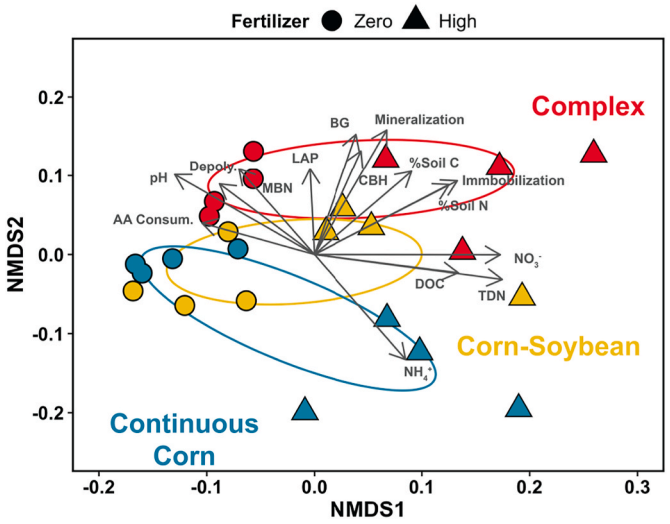

Fig. 3. Non-metric Multi-dimensional Scaling (NMDS) ordination for N flux rates, soil biogeochemical characteristics, and microbial enzyme activity and biomass with respect to cropping system complexity and fertilizer application. Longer vectors indicate stronger predictors, while shorter vectors indicate weaker predictors within the ordination space. Ellipses represent the standard deviation of the point scores for each group.

rates between fertilized and unfertilized plots in the continuous corn and corn-soybean systems. This suggests that complex cropping systems are more sensitive to external N inputs and respond by reducing organic N cycling to rates observed in lower complexity systems. We illustrate the overall differences between the two most contrasting treatments to highlight the variation in how fertilizer application and crop rotational complexity alter internal N cycling (Fig. 4).

Complex rotations, especially those that include a cover crop, can enhance soil C stocks by altering the timing and increasing the quantity and chemical diversity of residue inputs (King and Blesh, 2018; Syswerda et al., 2011; Tiemann and Grandy, 2015). Contributions to the SOM pool via crop biomass provide ample substrate quantity and the diversity of this residue increases substrate quality by providing more niches for microbial degradation (McDaniel et al., 2014a). We found that the complex and corn-soybean cropping systems had higher aboveground biomass than the continuous corn system (SI Table 3). Harvesting grain from a continuous corn system removes a large portion of biomass and crop N. Although residues were returned to the soil, corn has a higher CN ratio (50–60:1) than the other crops rotated in the corn-soybean and high complexity system, except for oat (70:1), which is grown simultaneously with clover (10–20:1). The higher complexity system likely provides larger quantities of organic N, and a greater variety of N-bearing molecules, that microbes can degrade and further depolymerize (Noll et al., 2019b; West and Post, 2002). Although there were no differences in the total amino acid pool size between the HFCC (High Fertilizer Continuous Corn) and ZFCR (Zero Fertilizer, Complex Rotations) treatments (SI Table 1), our study shows that gross depolymerization rates in the ZFCR system were nearly double that of the HFCC system (Fig. 1a). Furthermore, we found that pH was significantly lower in the HFCC treatment when compared to all other treatments (SI Fig. 1). High ammonium concentrations derived from mineral fertilizers can lower soil pH through nitrification by releasing hydrogen ions, thus acidifying the soil. Given that pH can inhibit microbial activity and SOM turnover (Averill and Waring, 2018; Kemmitt et al., 2006), lower depolymerization rates in this treatment may be driven by lower pH although the correlation between pH and depolymerization rates is rather weak ($p = 0.05$; $R^2 = 0.12$).

In the ZFCR treatment, amino acid consumption rates were nearly double that of depolymerization rates (Fig. 1a and b). This indicates that the microbial community consumes more free amino acids in the ZFCR system relative to the HFCC system, and this is mirrored in the size of the corresponding MBN pools, though this difference is likely attributed to differences in fertilizer rate. Carbon acquiring enzyme activities β-glucosaminidase and cellobiohydrolase were higher under more complex rotations but unaffected by N fertilization (Table 1), suggesting that complex rotations increase microbial investment in C-acquiring enzymes. We expected and generally observed that the ZFCR system has the highest rates of depolymerization and amino acid consumption to sustain microbial metabolic needs (Feng et al., 2018; Geisseler and Horwath, 2009; Noll et al., 2019a), and found that it also had the highest MBC and MBN compared to other treatments. Furthermore, under the most complex rotation, amino acid consumption was nearly three times higher in the unfertilized plots than in the fertilized plots (Fig. 1b). Thus, high fertilizer application rates reduce microbial demand for amino acids in complex cropping systems. Finally, amino acid mean residence time (MRT) in the HFCC is nearly four times greater than the MRT of the ZFRC. Taken together, these results show that amino acids cycle through the ZFCR system more rapidly which demonstrates that unfertilized, complex cropping systems can support high rates of internal N recycling (Fig. 1c).

On the other hand, amino acid consumption in the corn-soybean system was on the higher end of the observed spectrum within this

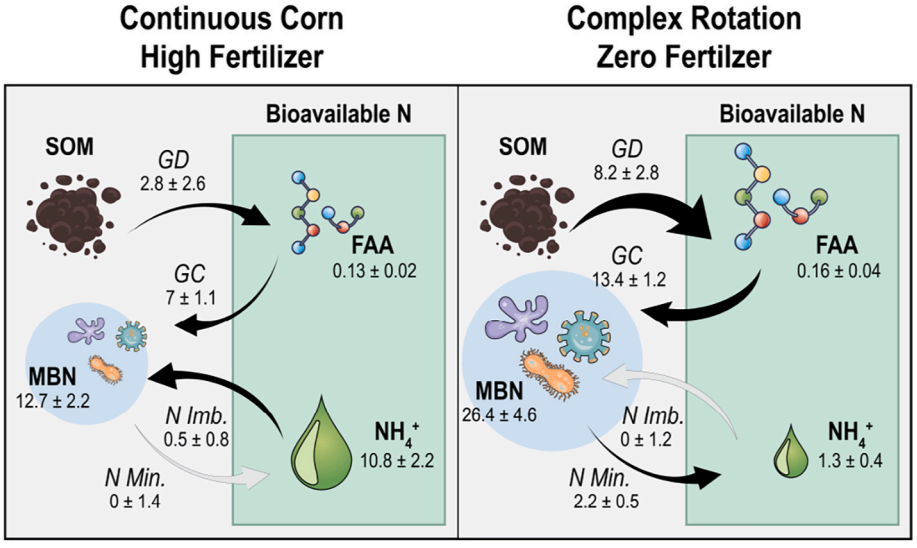

Fig. 4. Conceptual model depicting the changes in N pools and fluxes in the two most distinct treatments. The left panel shows pools and fluxes for the high fertilizer, continues corn (HFCC) treatment and the right panel shows the zero fertilizer, complex rotation (ZFCR) treatment. N pools are shown in bold and expressed in units of μg N g^{-1} dw soil. N fluxes are italicized and expressed in units of μg N g^{-1} dw soil d^{-1}. Pools and arrows are scaled by the comparison between treatments. Abbreviations: soil organic matter (SOM); free amino acids (FAA); microbial biomass N (MBN); ammonium (NH4+); gross depolymerization (GD); gross amino acid consumption (GC); N mineralization (N min.); N immobilization (Imb.). Light gray arrows indicate zero flux.

study and may be an indicator of a C-starved microbial community. Soil organic matter in long-term corn-soybean systems often declines, which Hall et al. (2019) suggest is due to a unique interaction between corn residue, soybean residue, and the microbial community (Huggins et al., 2007; Liebig et al., 2002; Poffenbarger et al., 2017). Corn residue inputs increase soil C decomposition via priming mechanisms, while the more labile soybean residue increases microbial biomass, further contributing to these priming effects. Thus, microbes in corn-soybean systems with high N fertilizer rates may be particularly C-starved and thus rely in part on amino acids as an accessible C source. However, these dynamics may be unique to corn-soybean cropping systems and other medium-complexity cropping systems may not exhibit the same organic N cycling dynamics. For example, incorporating a non-leguminous winter cover crop with a higher CN ratio than soy (e.g., rye) into a corn-soybean no-till system increases SOM, POM, and potentially mineralizable N (Moore et al., 2014).

Both cropping complexity and fertilization influenced microbial NH_4^+ mineralization, but not NH_4^+ immobilization (Fig. 2); only fertilization influenced immobilization rates. In the HFCC system, mineralization rates were essentially zero. In contrast in the ZFCR system, mineralization rates were nearly 10x higher than the HFCC system. Furthermore, the NH_4^+ pool size in the HFCC system was nearly 10x higher than the NH_4^+ pool in the ZFCR system, suggesting that the NH_4^+ pool in the HFCC system turns over more slowly relative to the ZFCR system. Yet, fertilization drove immobilization rates, with higher immobilization rates occurring in high fertilizer systems and we did not detect significant differences in NH_4^+ MRT between treatments. In general we might expect that NH_4^+ pool size would be larger in systems with higher mineralization rates (Booth et al., 2005), however these dynamics may be masked by the input of external fertilizers or may not reflect crop N demand and consumption. Furthermore, two of the three cropping systems in our study have legumes in rotation, which also contribute to the total bioavailable N pool via biological N fixation (BNF). Thus, the differences between NH_4^+ flux and pool size between systems may be attributed to the size and source of external N inputs, as well as the crops present in rotation. For instance, in the HFCC system a large portion of the NH_4^+ pool comes from fertilizer inputs that supports corn productivity, while organic N (e.g., amino acids) is the primary source of mineralized NH_4^+ in the ZFCR system. Our findings are in line with previous work that demonstrated elevated soil N pools in complex cropping systems, especially with the addition of leguminous cover crop (Drinkwater et al., 1998; Grandy and Robertson, 2007; McDaniel et al., 2014b). However, complex cropping systems with legumes in rotation may be susceptible to declines in bioavailable N under high inorganic N applications due to BNF downregulation (Schipanski and Drinkwater, 2012; Snapp et al., 2017). As such, growers may lose the benefits of internal N cycling in complex systems with high fertilizer rates.

Indicators of biogeochemical cycling exhibit a clear separation between continuous corn and complex cropping systems (Fig. 3). Our multivariate analysis shows that organic N flux, inorganic N flux, and variables that are associated with soil health metrics (e.g., enzyme activity, microbial biomass) track strongly with complex cropping systems. For example, our results indicate that microbial biomass C was higher in the unfertilized, complex cropping system than any other treatment combination (except the unfertilized, corn-soybean system) ($p = 0.02$), partially explaining the higher rates of amino acid cycling in the unfertilized, complex system. Microbial demand for C and N likely derive the rates of amino acid consumption, because amino acids are an easily accessible source of both C and N (Moe, 2013). However, even with lower microbial biomass C, the fertilized complex cropping system still demonstrated similar levels of NH_4^+ mineralization rates as the unfertilized complex system, which may be due to shifts in microbial N use efficiency as method of adjusting to resource imbalances. For example, Mooshammer et al. (2014b) found that microbes in N limited environments (e.g., organic horizons and plant litter) were very efficient at assimilating organic N into their biomass. However, crossing a stoichiometric C:N threshold where microbial growth is no longer constrained by N availability, but rather C availability, results in a release of excess N via mineralization (Mooshammer et al., 2014b). As such, complex cropping systems that receive fertilizer likely toe the line between C and N limited, depending on the timing of fertilizer application, thus, encouraging a shift in microbial N use efficiency under C limited circumstances (i.e., heavy fertilization).

We recognize that dichotomous fertilizer treatments allow us to examine potential responses of organic N cycling to N but may limit our capacity to derive from the results specific management recommendations. We also conducted our study exclusively in a no-till system that limits our ability to offer targeted management suggestions for different types of tillage. Yet, the total acreage of reduced tillage and no-tillage increased by 28% and 8%, respectively, from 2012 to 2017 in the United States, with most of the increase occurring in states situated in the corn belt (USDA National Agricultural Statistics Service, 2020). Given the increase in conservation tillage practices in recent years, our results provide valuable insights into soil responses in reduced tillage systems, specifically concerning organic N cycling. Our results show that no fertilization combined with increased cropping complexity may optimize internal N cycling relative to very high N fertilizer rates. However, future research should investigate a gradient of fertilizer rates coupled with high rotational complexity to understand better how to balance internal and external sources of N to promote N use efficiency.

In our study system, we found that complex rotations with reduced fertilizer promotes high rates of organic N cycling while still maintaining similar mineralization rates as high fertilizer systems. However, the inclusion of high inorganic fertilizer inputs tempers organic N transformations, thus undermining the benefit of internal N cycling that complex crop rotations provide. Our results may help explain previous work from the long-term, crop diversity study that ascertain complex rotations with minimal fertilizer can still produce crop yields that are similar to fertilized, monoculture systems (Sindelar et al., 2016). For example, Sindelar et al. (2016) found that total crop N uptake decreases with increasing rotation complexity when fertilizer inputs increase from 90 to 180 kg N ha^{-1}. The reduction in crop N uptake in complex systems under high fertilization suggests that the crops are less dependent on the external N source, and more dependent on organic N sources. Moreover, increased inorganic N may facilitate shifts in microbial resource allocation, thus slowing organic N recycling and promoting mineralization (Mooshammer et al., 2014a).

5. Conclusions

The results of our study suggest that a balance between low fertilizer inputs and high rotational complexity can increase internal N cycling. However, in order to develop specific regional management recommendations future work should use a wider range of N fertilizer rates, study sites, and agronomic management strategies (e.g., different cropping and tillage systems). Finding the optimal balance between external N application rates across a wide range of agronomic conditions will provide farmers economic benefits and reduce environmental N losses.

Declaration of competing interest

The authors declare that they have no known competing financial interests or personal relationships that could have appeared to influence the work reported in this paper.

Data availability

Data will be made available on request.

Acknowledgments

We would like to thank S. Greenwood, B. Balstad, and D. Thibault for their contributions toward method development. We thank A.B. Daly for valuable feedback on the manuscript. Finally, we would like to thank S. Swanson, B. Fann, and D. Walla for maintaining the facilities at the Eastern Nebraska Research and Extension Center. The research was funded by the USDA NIFA Agriculture and Food Research initiative (Grant 2017- 67013-26254).

Appendix A. Supplementary data

Supplementary data to this article can be found online at https://doi.org/10.1016/j.soilbio.2022.108911.

References

Anderson, M.J., Walsh, D.C.I., 2013. PERMANOVA , ANOSIM , and the Mantel Test in the Face of Heterogeneous Dispersions : what Null Hypothesis Are You Testing ? Author (S): Marti J . Anderson and Daniel C . I . Walsh Published by, vol. 83. Wiley on behalf of the Ecological Society of America Stable, pp. 557–574.

Averill, C., Waring, B., 2018. Nitrogen limitation of decomposition and decay: how can it occur? Global Change Biology 24, 1417–1427. https://doi.org/10.1111/gcb.13980.

Bach, C.E., Warnock, D.D., Van Horn, D.J., Weintraub, M.N., Sinsabaugh, R.L., Allison, S. D., German, D.P., 2013. Measuring phenol oxidase and peroxidase activities with pyrogallol, l-DOPA, and ABTS: effect of assay conditions and soil type. Soil Biology and Biochemistry 67, 183–191. https://doi.org/10.1016/j.soilbio.2013.08.022.

Bardgett, R.D., Streeter, T.C., Bol, R., 2003. Soil Microbes Compete Effectively with Plants for Organic-Nitrogen Inputs to Temperate Grasslands 84, 1277–1287.

Bates, D., Mächler, M., Bolker, B., Walker, S., 2015. Fitting linear mixed-effects models using lme4. Journal of Statistical Software 67. https://doi.org/10.18637/jss.v067.i01.

Baumhardt, R.L., Stewart, B.A., Sainju, U.M., 2015. North American soil degradation: processes, practices, and mitigating strategies. Sustainability 7, 2936–2960. https://doi.org/10.3390/su7032936.

Bodirsky, B.L., Popp, A., Weindl, I., Dietrich, J.P., Rolinski, S., Scheiffele, L., Schmitz, C., Lotze-Campen, H., 2012. N2O emissions from the global agricultural nitrogen cycle-current state and future scenarios. Biogeosciences 9, 4169–4197. https://doi.org/10.5194/bg-9-4169-2012.

Booth, M.S., Stark, J.M., Rastetter, E., 2005. Controls on nitrogen cycling in terrestrial ecosystems: a synthetic analysis of literature data. Ecological Monographs 75, 139–157. https://doi.org/10.1890/03-8021.

Bowles, T.M., Jilling, A., Morán-Rivera, K., Schnecker, J., Grandy, A.S., 2022. Crop rotational complexity affects plant-soil nitrogen cycling during water deficit. Soil Biology and Biochemistry 166. https://doi.org/10.1016/j.soilbio.2022.108552.

Bowles, T.M., Mooshammer, M., Socolar, Y., Calderón, F., Cavigelli, M.A., Culman, S.W., Deen, W., Drury, C.F., Garcia y Garcia, A., Gaudin, A.C.M., Harkcom, W.S., Lehman, R.M., Osborne, S.L., Robertson, G.P., Salerno, J., Schmer, M.R., Strock, J., Grandy, A.S., 2020. Long-term evidence shows that crop-rotation diversification increases agricultural resilience to adverse growing conditions in north America. One Earth 2, 284–293. https://doi.org/10.1016/j.oneear.2020.02.007.

Chen, W., Yang, X., Hegeman, A.D., Gray, W.M., Cohen, J.D., 2010. Microscale analysis of amino acids using gas chromatography – mass spectrometry after methyl chloroformate derivatization. Journal of Chromatography B 878, 2199–2208. https://doi.org/10.1016/j.jchromb.2010.06.027.

Dexter, A.R., Richard, G., Arrouays, D., Czyz, E.A., Jolivet, C., Duval, O., 2008. Complexed organic matter controls soil physical properties. Geoderma 144, 620–627. https://doi.org/10.1016/j.geoderma.2008.01.022.

Doran, J.W., Zeiss, M.R., 2000. Soil health and sustainability: managing the biotic component of soil quality. Applied Soil Ecology 15, 3–11. https://doi.org/10.1016/S0929-1393(00)00067-6.

Drinkwater, L.E., Snapp, S.S., 2007. Nutrients in agroecosystems: rethinking the management paradigm. Advances in Agronomy 92, 163–186. https://doi.org/10.1016/S0065-2113(04)92003-2.

Drinkwater, L.E., Wagoner, P., Sarrantonio, M., 1998. Legume-based cropping systems have reuced carbon and nitrogen losses. Nature 396, 262–265. https://doi.org/10.1038/24376.

Farzadfar, S., Knight, J.D., Congreves, K.A., 2021. Soil organic nitrogen: an overlooked but potentially significant contribution to crop nutrition. Plant and Soil 462, 7–23. https://doi.org/10.1007/s11104-021-04860-w.

Feller, C., Beare, M.H., 1997. Physical control of soil organic matter dynamics in the tropics. Geoderma 79, 69–116. https://doi.org/10.1016/S0016-7061(97)00039-6.

Feng, G., Xie, T., Wang, X., Bai, J., Tang, L., Zhao, H., Wei, W., Wang, M., Zhao, Y., 2018. Metagenomic analysis of microbial community and function involved in cd-contaminated soil. BMC Microbiology 18, 1–13. https://doi.org/10.1186/s12866-018-1152-5.

Geisseler, D., Horwath, W.R., 2009. Relationship between carbon and nitrogen availability and extracellular enzyme activities in soil. Pedobiologia 53, 87–98. https://doi.org/10.1016/j.pedobi.2009.06.002.

Geisseler, D., Horwath, W.R., 2008. Regulation of extracellular protease activity in soil in response to different sources and concentrations of nitrogen and carbon. Soil Biology and Biochemistry 40, 3040–3048. https://doi.org/10.1016/j.soilbio.2008.09.001.

Geisseler, D., Horwath, W.R., Doane, T.A., 2009. Significance of organic nitrogen uptake from plant residues by soil microorganisms as affected by carbon and nitrogen availability. Soil Biology and Biochemistry 41, 1281–1288. https://doi.org/10.1016/j.soilbio.2009.03.014.

German, D.P., Weintraub, M.N., Grandy, A.S., Lauber, C.L., Rinkes, Z.L., Allison, S.D., 2011. Optimization of hydrolytic and oxidative enzyme methods for ecosystem studies. Soil Biology and Biochemistry 43, 1387–1397. https://doi.org/10.1016/j.soilbio.2011.03.017.

Grandy, A.S., Robertson, G.P., 2007. Land-use intensity effects on soil organic carbon accumulation rates and mechanisms. Ecosystems 10, 58–73. https://doi.org/10.1007/s10021-006-9010-y.

Hall, S.J., Russell, A.E., Moore, A.R., 2019. Do corn-soybean rotations enhance decomposition of soil organic matter? Plant and Soil 444, 427–442. https://doi.org/10.1007/s11104-019-04292-7.

Hood-Nowotny, R., Umana, N.H.-N., Inselbacher, E., Oswald- Lachouani, P., Wanek, W., 2010. Alternative methods for measuring inorganic, organic, and total dissolved nitrogen in soil. Soil Science Society of America Journal 74, 1018–1027. https://doi.org/10.2136/sssaj2009.0389.

Hu, G., He, H., Zhang, W., Zhao, J., Cui, J., Li, B., Zhang, X., 2016. The transformation and renewal of soil amino acids induced by the availability of extraneous C and N. Soil Biology and Biochemistry 96, 86–96. https://doi.org/10.1016/j.soilbio.2016.01.019.

Huggins, D.R., Allmaras, R.R., Clapp, C.E., Lamb, J.A., Randall, G.W., 2007. Corn-soybean sequence and tillage effects on soil carbon dynamics and storage. Soil Science Society of America Journal 71, 145–154. https://doi.org/10.2136/sssaj2005.0231.

Hurisso, T.T., Moebius-Clune, D.J., Culman, S.W., Moebius-Clune, B.N., Thies, J.E., van Es, H.M., 2018. Soil protein as a rapid soil health indicator of potentially available organic nitrogen. Ael 3. https://doi.org/10.2134/ael2018.02.0006, 0.

Hušek, P., 1991. Rapid derivatization and gas chromatographic determination of amino acids. Journal of Chromatography A 552, 289–299. https://doi.org/10.1016/S0021-9673(01)95945-X.

Jilling, A., Kane, D., Williams, A., Yannarell, A.C., Davis, A., Jordan, N.R., Koide, R.T., Mortensen, D.A., Smith, R.G., Snapp, S.S., Spokas, K.A., Stuart Grandy, A., 2020. Rapid and distinct responses of particulate and mineral-associated organic nitrogen to conservation tillage and cover crops. Geoderma 359, 114001. https://doi.org/10.1016/j.geoderma.2019.114001.

Jones, D.L., Kielland, K., 2002. Soil amino acid turnover dominates the nitrogen flux in permafrost-dominated taiga forest soils. Soil Biology and Biochemistry 34, 209–219. https://doi.org/10.1016/S0038-0717(01)00175-4.

Jones, D.L., Owen, A.G., Farrar, J.F., 2002. Simple method to enable the high resolution determination of total free amino acids in soil solutions and soil extracts. Soil Biology and Biochemistry 34, 1893–1902. https://doi.org/10.1016/S0038-0717(02)00203-1.

Kandeler, E., Gerber, H., 1988. Short-term assay of soil urease activity using colorimetric determination of ammonium. Biology and Fertility of Soils 6, 68–72. https://doi.org/10.1007/BF00257924.

Kemmitt, S.J., Wright, D., Goulding, K.W.T., Jones, D.L., 2006. pH regulation of carbon and nitrogen dynamics in two agricultural soils. Soil Biology and Biochemistry 38, 898–911. https://doi.org/10.1016/j.soilbio.2005.08.006.

Khan, S.A., Mulvaney, R.L., Ellsworth, T.R., Boast, C.W., 2007. The myth of nitrogen fertilization for soil carbon sequestration. Journal of Environmental Quality 36, 1821–1832. https://doi.org/10.2134/jeq2007.0099.

Kibblewhite, M.G., Ritz, K., Swift, M.J., 2008. Soil health in agricultural systems. Philosophical Transactions of the Royal Society of London Series B Biological Sciences 363, 685–701. https://doi.org/10.1098/rstb.2007.2178.

King, A.E., Ali, G.A., Gillespie, A.W., Wagner-Riddle, C., 2020. Soil organic matter as catalyst of crop resource capture. Frontiers in Environmental Science 8, 1–8. https://doi.org/10.3389/fenvs.2020.00050.

King, A.E., Blesh, J., 2018. Crop rotations for increased soil carbon: perenniality as a guiding principle: Perenniality. Ecological Applications 28, 249–261. https://doi.org/10.1002/eap.1648.

Kirkham, D., Bartholomew, W.V., 1954. Equations for following nutrient transformations in soil, utilizing tracer Data1. Soil Science Society of America Journal 18, 33. https://doi.org/10.2136/sssaj1954.03615995001800010009x.

Lenth, R.V., 2020. Emmeans: Estimated Marginal Means, Aka Least-Squares Means. R package version 1.4.8.

Liebig, M.A., Varvel, G.E., Doran, J.W., Wienhold, B.J., 2002. Crop sequence and nitrogen fertilization effects on soil properties in the western corn belt. Soil Science Society of America Journal 66, 596–601. https://doi.org/10.2136/sssaj2002.5960.

Mahal, N.K., Osterholz, W.R., Miguez, F.E., Poffenbarger, H.J., Sawyer, J.E., Olk, D.C., Archontoulis, S.V., Castellano, M.J., 2019. Nitrogen fertilizer suppresses mineralization of soil organic matter in maize agroecosystems. Frontiers in Ecology and Evolution 7. https://doi.org/10.3389/fevo.2019.00059.

McDaniel, M.D., Grandy, A.S., Tiemann, L.K., Weintraub, M.N., 2014a. Crop rotation complexity regulates the decomposition of high and low quality residues. Soil Biology and Biochemistry 78, 243–254. https://doi.org/10.1016/j.soilbio.2014.07.027.

McDaniel, M.D., Tiemann, L.K., Grandy, A.S., 2014b. Does agricultural crop diversity enhance soil microbial biomass and organic matter dynamics? A meta-analysis. Ecological Applications 24, 560–570. https://doi.org/10.1890/13-0616.1.

Moe, L.A., 2013. Amino acids in the rhizosphere: from plants to microbes. American Journal of Botany 100, 1692–1705. https://doi.org/10.3732/ajb.1300033.

Moore, E.B., Wiedenhoeft, M.H., Kaspar, T.C., Cambardella, C.A., 2014. Rye cover crop effects on soil quality in No-till corn silage-soybean cropping systems. Soil Science Society of America Journal 78, 968–976. https://doi.org/10.2136/sssaj2013.09.0401.

Moorhead, D.L., Sinsabaugh, R.L., 2006. A theoretical model of litter decay and microbial interaction. Ecology 76, 151–174. https://doi.org/10.1890/07-1861.1.

Mooshammer, M., Grandy, A.S., Calderón, F., Culman, S., Deen, B., Drijber, R.A., Dunfield, K., Jin, V.L., Lehman, R.M., Osborne, S.L., Schmer, M., Bowles, T.M., 2022. Microbial feedbacks on soil organic matter dynamics underlying the legacy effect of diversified cropping systems. Soil Biology and Biochemistry 167. https://doi.org/10.1016/j.soilbio.2022.108584.

Mooshammer, M., Wanek, W., Hammerle, I., Fuchslueger, L., Hofhansl, F., Knoltsch, A., Schnecker, J., Takriti, M., Watzka, M., Wild, B., Keiblinger, K.M., Zechmeister-Boltenstern, S., Richter, A., 2014a. Adjustment of microbial nitrogen use efficiency to carbon:nitrogen imbalances regulates soil nitrogen cycling. Nature Communications 5, 3694. https://doi.org/10.1038/ncomms4694.

Mooshammer, M., Wanek, W., Schnecker, J., Wild, B., Leitner, S., Hofhansl, F., Blochl, A., Hammerle, I., Frank, A.H., Fuchslueger, L., Keiblinger, K.M., Zechmeister-Boltenstern, S., Richter, A., 2012. Stoichiometric controls of nitrogen and phosphorus cycling in decomposing beech leaf litter. Ecology 93, 770–782. https://doi.org/10.1890/11-0721.1.

Mooshammer, M., Wanek, W., Zechmeister-Boltenstern, S., Richter, A., 2014b. Stoichiometric imbalances between terrestrial decomposer communities and their resources: mechanisms and implications of microbial adaptations to their resources. Frontiers in Microbiology 5, 1–10. https://doi.org/10.3389/fmicb.2014.00022.

Näsholm, T., Huss-Danell, K., Högberg, P., 2000. Uptake of organic nitrogen in the field by four agriculturally important plant species. Ecology 81, 1155–1161. https://doi.org/10.1890/0012-9658(2000)081[1155:UOONIT]2.0.CO;2.

Neff, J.C., Townsend, A.R., Gleixner, G., Lehman, S.J., Turnbull, J., Bowman, W.D., 2002. Variable effects of nitrogen additions on the stability and turnover of soil carbon. Nature 419, 915–917. https://doi.org/10.1038/Nature01136.

Noll, L., Zhang, S., Wanek, W., 2019a. Novel high-throughput approach to determine key processes of soil organic nitrogen cycling: gross protein depolymerization and microbial amino acid uptake. Soil Biology and Biochemistry 130, 73–81. https://doi.org/10.1016/j.soilbio.2018.12.005.

Noll, L., Zhang, S., Zheng, Q., Hu, Y., Wanek, W., 2019b. Wide-spread limitation of soil organic nitrogen transformations by substrate availability and not by extracellular enzyme content. Soil Biology and Biochemistry 133, 37–49. https://doi.org/10.1016/j.soilbio.2019.02.016.

Norris, C.E., Congreves, K.A., 2018. Alternative management practices improve soil health indices in intensive vegetable cropping systems: a review. Frontiers in Environmental Science 6. https://doi.org/10.3389/fenvs.2018.00050.

Oksanen, J., Blanchet, F.G., Friendly, M., Kindt, R., Legendre, P., McGlinn, D., Minchin, P.R., O'Hara, R.B., Simpson, G.L., Solymos, P., Stevens, M.H.H., Szoecs, E., Wagner, H., 2020. Vegan: Community Ecology Package. R Package Version 2, pp. 5–6.

Persson, J., Näsholm, T., 2001. Amino acid uptake: a widespread ability among boreal forest plants. Ecology Letters 4, 434–438. https://doi.org/10.1046/j.1461-0248.2001.00260.x.

Poeplau, C., Don, A., 2015. Carbon sequestration in agricultural soils via cultivation of cover crops - a meta-analysis. Agriculture, Ecosystems & Environment 200, 33–41. https://doi.org/10.1016/j.agee.2014.10.024.

Poffenbarger, H.J., Barker, D.W., Helmers, M.J., Miguez, F.E., Olk, D.C., Sawyer, J.E., Six, J., Castellano, M.J., 2017. Maximum soil organic carbon storage in Midwest U.S. cropping systems when crops are optimally nitrogen-fertilized. PLoS One 12, 1–17. https://doi.org/10.1371/journal.pone.0172293.

R Core Team, 2020. R: A Language and Environment for Statistical Computing. R Foundation for Statistical Computing. https://www.R-project.org/.

Schimel, J.P., Bennett, J., 2004. Nitrogen mineralization: challenges of a changing paradigm. Ecology 85, 591–602. https://doi.org/10.1890/03-8002.

Schipanski, M.E., Drinkwater, L.E., 2012. Nitrogen fixation in annual and perennial legume-grass mixtures across a fertility gradient. Plant and Soil 357, 147–159. https://doi.org/10.1007/s11104-012-1137-3.

Sindelar, A.J., Schmer, M.R., Jin, V.L., Wienhold, B.J., Varvel, G.E., 2016. Crop rotation affects corn, grain sorghum, and Soybean yields and nitrogen recovery. Agronomy Journal 108, 1592–1602. https://doi.org/10.2134/agronj2016.01.0005.

Six, J., Paustian, K., Elliott, E.T., Combrink, C., 2000. Soil structure and organic matter I. Distribution of aggregate-size classes and aggregate-associated carbon. Soil Science Society of America Journal 64, 681–689. https://doi.org/10.2136/sssaj2000.642681x.

Smith, R.G., Gross, K.L., Robertson, G.P., 2008. Effects of crop diversity on agroecosystem function: crop yield response. Ecosystems 11, 355–366. https://doi.org/10.1007/s10021-008-9124-5.

Snapp, S., Wilke, B., Gentry, L.E., Zoellner, D., 2017. Compost legacy down-regulates biological nitrogen fixation in a long-term field experiment. Agronomy Journal 109, 2662–2669. https://doi.org/10.2134/agronj2017.03.0152.

Snapp, S.S., Fortuna, A.M., 2003. Predicting nitrogen availability in irrigated potato systems. HortTechnology 13, 598–604. https://doi.org/10.21273/horttech.13.4.0598.

Syswerda, S.P., Corbin, A.T., Mokma, D.L., Kravchenko, A.N., Robertson, G.P., 2011. Agricultural management and soil carbon storage in surface vs. Deep layers. Soil Science Society of America Journal 75, 92–101. https://doi.org/10.2136/sssaj2009.0414.

Tenorio, F.A.M., McLellan, E.L., Eagle, A.J., Cassman, K.G., Andersen, D., Krausnick, M., Oaklund, R., Thorburn, J., Grassini, P., 2020. Benchmarking impact of nitrogen inputs on grain yield and environmental performance of producer fields in the western US Corn Belt. Agriculture, Ecosystems & Environment 294, 106865. https://doi.org/10.1016/j.agee.2020.106865.

Tiemann, L.K., Grandy, A.S., 2015. Mechanisms of soil carbon accrual and storage in bioenergy cropping systems. GCB Bioenergy 7, 161–174. https://doi.org/10.1111/gcbb.12126.

Tiemann, L.K., Grandy, A.S., Atkinson, E.E., Marin-Spiotta, E., Mcdaniel, M.D., 2015. Crop rotational diversity enhances belowground communities and functions in an agroecosystem. Ecology Letters 18, 761–771. https://doi.org/10.1111/ele.12453.

USDA National Agricultural Statistics Service, 2020. Land Use Practice Results from the 2017 Census of Agriculture. www.nass.usda.gov/AgCensus.

Vance, E.D., Brookes, P.C., Jenkinson, D.S., 1987. Microbial biomass measurements in forest soils: the use of the chloroform fumigation-incubation method in strongly acid soils. Soil Biology and Biochemistry 19, 697–702. https://doi.org/10.1016/0038-0717(87)90051-4.

Velazquez, E., Mueller, N.D., Billen, G., Lassaletta, L., Bouwman, L., Garnier, J., Gerber, J.S., 2016. Nitrogen use in the global food system: past trends and future trajectories of agronomic performance, pollution, trade, and dietary demand. Environmental Research Letters 11, 095007. https://doi.org/10.1088/1748-9326/11/9/095007.

Vinolas, L.C., Healey, J.R., Jones, D.L., 2001. Kinetics of soil microbial uptake of free amino acids. Biology and Fertility of Soils 33, 67–74. https://doi.org/10.1007/s003740000291.

Vitousek, P.M., Aber, J.D., Howarth, R.W., Likens, G., Matson, P., Schindler, D., Schlesinger, W., Tilman, D., 1997. Human alteration of the global nitrogen cycle: sources and consequences. Ecological Applications 7, 737–750. https://doi.org/10.1890/1051-0761(1997)007[0737:HAOTGN]2.0.CO;2.

Wanek, W., Mooshammer, M., Blöchl, A., Hanreich, A., Richter, A., 2010. Determination of gross rates of amino acid production and immobilization in decomposing leaf litter by a novel15N isotope pool dilution technique. Soil Biology and Biochemistry 42, 1293–1302. https://doi.org/10.1016/j.soilbio.2010.04.001.

Wardle, D.A., Bardgett, R.D., Klironomos, J.N., Setälä, H., Van Der Putten, W.H., Wall, D. H., 2004. Ecological linkages between aboveground and belowground biota. Science 304, 1629–1633. https://doi.org/10.1126/science.1094875.

West, T.O., Post, W.M., 2002. Soil organic carbon sequestration rates by tillage and crop rotation. Soil Science Society of America Journal 66, 1930–1946. https://doi.org/10.2136/sssaj2002.1930.

Wickham, H., 2020. ggplot2: Elegant Graphics for Data Analysis.

Wild, B., Schnecker, J., Bárta, J., Čapek, P., Guggenberger, G., Hofhansl, F., Kaiser, C., Lashchinsky, N., Mikutta, R., Mooshammer, M., Šantrůčková, H., Shibistova, O., Urich, T., Zimov, S.A., Richter, A., 2013. Nitrogen dynamics in turbic cryosols from siberia and Greenland. Soil Biology and Biochemistry 67, 85–93. https://doi.org/10.1016/j.soilbio.2013.08.004.

Yan, M., Pan, G., Lavallee, J.M., Conant, R.T., 2019. Rethinking sources of nitrogen to cereal crops. Global Change Biology 1–9. https://doi.org/10.1111/gcb.14908.

Yu, Z.S., Northup, R.R., Dahlgren, R.A., 1994. Determination of dissolved organic nitrogen using persulfate oxidation and conductimetric quantification of nitrate-nitrogen. Communications in Soil Science and Plant Analysis. https://doi.org/10.1080/00103629409369255.

Zheng, L., Chen, H., Wang, Y., Mao, Q., Zheng, M., Su, Y., Xiao, K., Wang, K., Li, D., 2020. Responses of soil microbial resource limitation to multiple fertilization strategies. Soil and Tillage Research 196, 104474. https://doi.org/10.1016/j.still.2019.104474.